Molecular Therapy
Oncolytics
Original Article

A Screened GPR1 Peptide Exerts Antitumor Effects on Triple-Negative Breast Cancer

Chen Huang,[1,3,6] Xiao-Yong Dai,[1,6] Jia-Xuan Cai,[2,6] Jie Chen,[1] Bao Bei Wang,[1] Wen Zhu,[1,5] Esther Wang,[4] Wei Wei,[2] and Jian V. Zhang[1,3,5]

[1]Center for Energy Metabolism and Reproduction, Institute of Biomedicine and Biotechnology, Shenzhen Institute of Advanced Technology, Chinese Academy of Sciences, Shenzhen, Guangdong 518055, China; [2]Peking University Shen Zhen Hospital, Shen Zhen, Guangdong, 518036, China; [3]Department of Clinical Pharmacy and Translational Medicine , School of Pharmacy and Biomedicine, Shenzhen Institutes of Advanced Technology, Chinese Academy of Sciences, Shenzhen, China; [4]Biological Sciences Collegiate Division, University of Chicago, Chicago, IL, USA; [5]Shenzhen College of Advanced Technology, University of Chinese Academy of Sciences, Shenzhen

The adipokine chemerin has been considered an important regulator of tumor immune surveillance. Chemerin recruits leukocytes through the receptor CMKLR1 to improve clinical outcomes of tumors and overall patient survival, but the role of GPR1 in tumors has not been widely investigated. Here, we found that GPR1 expression is elevated in breast cancer—especially triple-negative breast cancer (TNBC) tissues and cell lines. Herein, we screened a phage display peptide library to identify LRH7-G5, a peptide antagonist that blocks chemerin/GPR1 signaling. This peptide performed as an anticancer agent to suppress the proliferation of the TNBC cell lines MDA-MB-231 and HCC1937 but has little effect on T47D cells. LRH7-G5 treatment significantly blocked tumor growth in a TNBC cell-bearing orthotopic mouse model. Last, our results showed that this peptide's antitumor role is mediated through the PI3K/AKT signaling pathway. In conclusion, these data collectively suggest that the chemerin receptor GPR1 is a novel target for controlling TNBC progression and establish peptide LRH7-G5 as a new therapeutic agent for suppressing TNBC tumor growth.

INTRODUCTION

Globally, breast cancer (BC) is the most common malignancy and the leading cause of cancer-related mortality in women worldwide.[1,2] Based on the presence/absence of the estrogen receptor (ER), the progesterone receptor (PR), and human epidermal growth factor-2 (HER2), breast cancer subtypes can be classified into the following subtypes: luminal A, luminal B, HER2-overexpressing, and triple-negative[3,4] Triple-negative breast cancer (TNBC) tumors are often more aggressive, are less sensitive to typical endocrine therapies, have a poorer prognosis, and have a higher rate of distinct recurrence than tumors of other subtypes.[5–7] The triple-negative subtype does not respond to conventional anti-hormone or molecular targeted therapies and therefore has limited treatment options. Thus, TNBC therapies constitute a significant unmet medical need.

G protein-coupled receptor 1 (GPR1), a receptor for chemokine-like peptide (chemerin), plays an essential role in metabolism and reproduction.[8,9] Chemerin is an adipokine and is secreted mainly from white adipose tissue. Activation of GPR1 by chemerin results in intracellular calcium release, inhibition of cyclic adenosine monophosphate (cAMP) accumulation, and phosphorylation of the p42-p44 MAP kinases through the Gi class of heterotrimeric G proteins.[10,11] GPR1 has also been identified as a coreceptor for the entry of HIV-1 variants and mutants into target cells.[12] Recently, GPR1 was reported to promote cancer cell proliferation and invasion in choriocarcinoma cells and gastric cancer cells,[13] which prompted us to focus on the role of GPR1 in tumors. Here, we found that GPR1 was highly expressed in breast cancer tissue and cell lines, especially in TNBC cell lines. Analysis of data from The Cancer Genome Atlas (TGCA) indicated a close correlation between TNBC and GPR1. To investigate the role of GPR1 in breast cancer, we screened the Ph.D.-7 random phage library to identify the GPR1-specific peptide LRH7-G5, which competes with chemerin to block chemerin/GPR1 signaling. As expected, this peptide directly inhibited the proliferation of the TNBC cell lines MDA-MB-231 and HCC1937 and suppressed tumor growth in a dose-dependent manner but did not affect T47D cells. We also provided evidence that this peptide's antitumor role is mediated through PI3K/AKT signaling.

RESULTS

The Expression Status of GPR1 Is Related to TNBC Progression

To determine the relationship between GPR1 and breast cancer progression, we examined GPR1 expression in breast cancer cell lines and breast cancer tissue. The GPR1 level was significantly elevated in TNBC, as shown by its increased RNA and protein expression levels

Received 26 February 2020; accepted 20 August 2020;
https://doi.org/10.1016/j.omto.2020.08.013.

[6]These authors contributed equally to this work.

Correspondence: Jian V. Zhang, Center for Energy Metabolism and Reproduction, Institute of Biomedicine and Biotechnology, Shenzhen Institute of Advanced Technology, Chinese Academy of Sciences, Shenzhen, Guangdong 518055, China.
E-mail: jian.zhang@siat.ac.cn
Correspondence: Wei Wei, Peking University Shen Zhen Hospital, Shen Zhen, Guangdong 518036, China.
E-mail: rxwei1123@163.com

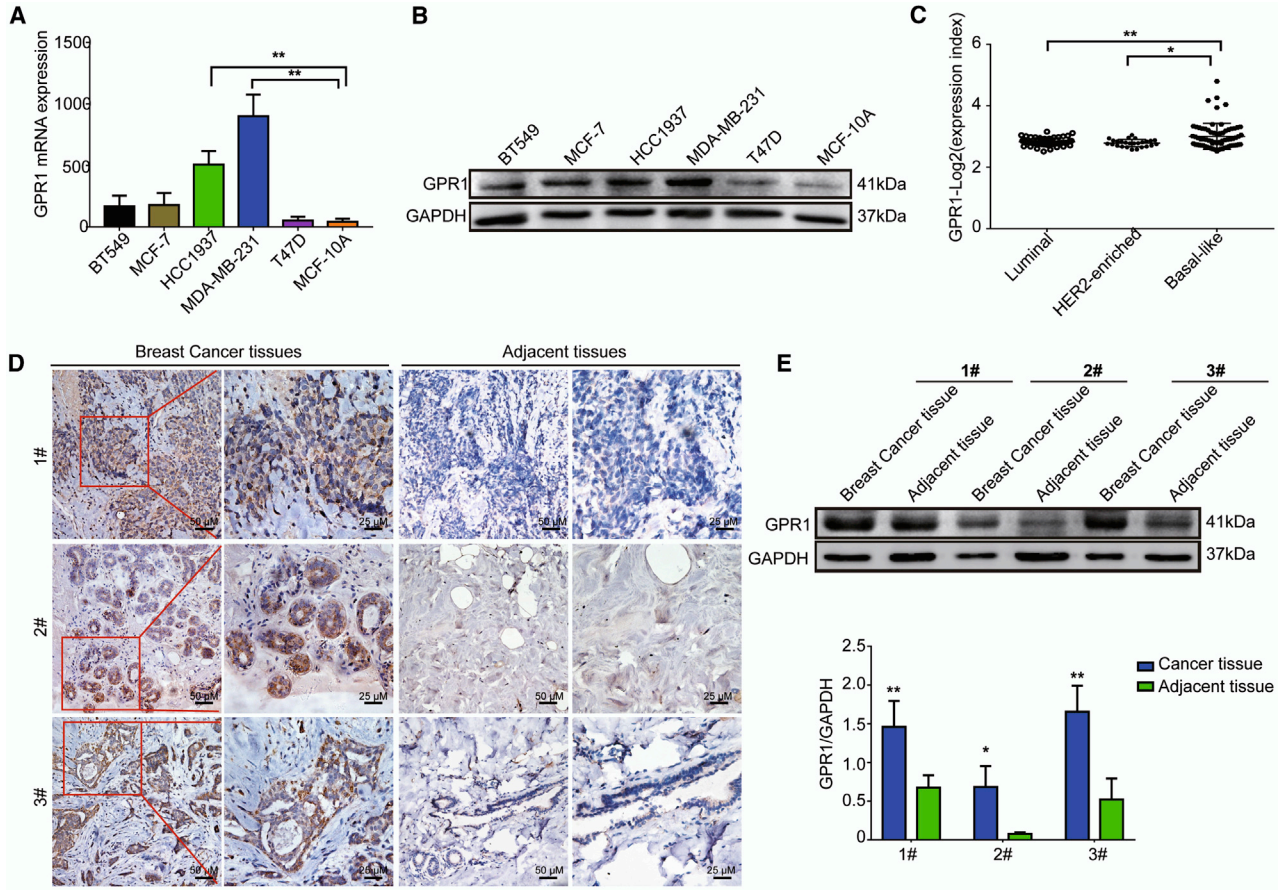

Figure 1. The Expression Status of GPR1 Is Related with Breast Cancer Progression

(A and B) Expression of GPR1 in breast cancer cell lines was measured by real-time RT-PCR (A) and western blot (B). P value is compared with MCF-10A, $^{**}p < 0.001$ (C) Scatter dot plots shown GPR1 expression levels in breast cancer cell lines from GEO datasets:GSE41313. Luminal (n = 51), Her2-enriched (n = 26), and basal-like (n = 70), one-way ANOVA was performed for significance. (D) GPR1 staining in breast cancer tissue and adjacent tissue. (E) GPR1 protein level in breast cancer tissue. One-way ANOVA was performed for significance. $^{*}p < 0.05$, $^{**}p < 0.001$ versus adjacent samples. The results are representative of three independent experiments and are expressed as the mean ± SD.

in HCC1937 and MDA-MB-231 cell lines (Figures 1A and 1B). Furthermore, the analysis of breast cancer cell lines from a public microarray dataset:GSE41313[14] confirmed a correlation between the GPR1 level and a basal-like subtype in cancer cell lines (Figure 1C). We also found that endogenous expression of GPR1 was positively associated with breast cancer tissues (Figures 1D and 1E). Together, these data suggest that GPR1 may be clinically significant for characterizing breast cancer progression, especially the development of TNBC.

The Selected Peptides Specifically Block Chemerin/GPR1 Signaling

To further investigate the role of GPR1 in breast cancer, we evaluated a Ph.D.-7 Phage Display Peptide Library in HEK293 $GPR1^{+/+}$ cells to identify peptides binding GPR1. Figure S1A shows a schematic of the phage display workflow. After five rounds of evaluating clones for binding specificity, the 6 phage clones with high binding ability were finally identified, among which LRH7-G5 showed the highest affinity (Figure 2A). The binding affinities of LRH7-G5 were determined by the binding kinetics, which were evaluated using the dissociation constant (KD) values in the GPR1-expressing cell line and the TNBC cell lines MDA-MB-231 and HCC1937 (Figures S1B and S1C), and were validated by confirming colocalization of the peptides and GPR1 in breast cancer cell lines (Figure 2B).

To further examine the effect of LRH7-G5 on GPR1 signaling, we utilized cAMP and calcium mobilization assays. As shown in Figures 2C and 2D, chemerin suppressed forskolin-induced cAMP release, and this effect was dose-dependently abolished by LRH7-G5 treatment. A similar result was observed in the calcium release assay. In these GPR1-expressing cells, LRH7-G5 treatment significantly decreased chemerin-induced calcium mobilization. In contrast, this peptide did not affect HEK293 pcDNA cells (Figure 2D). Most importantly,

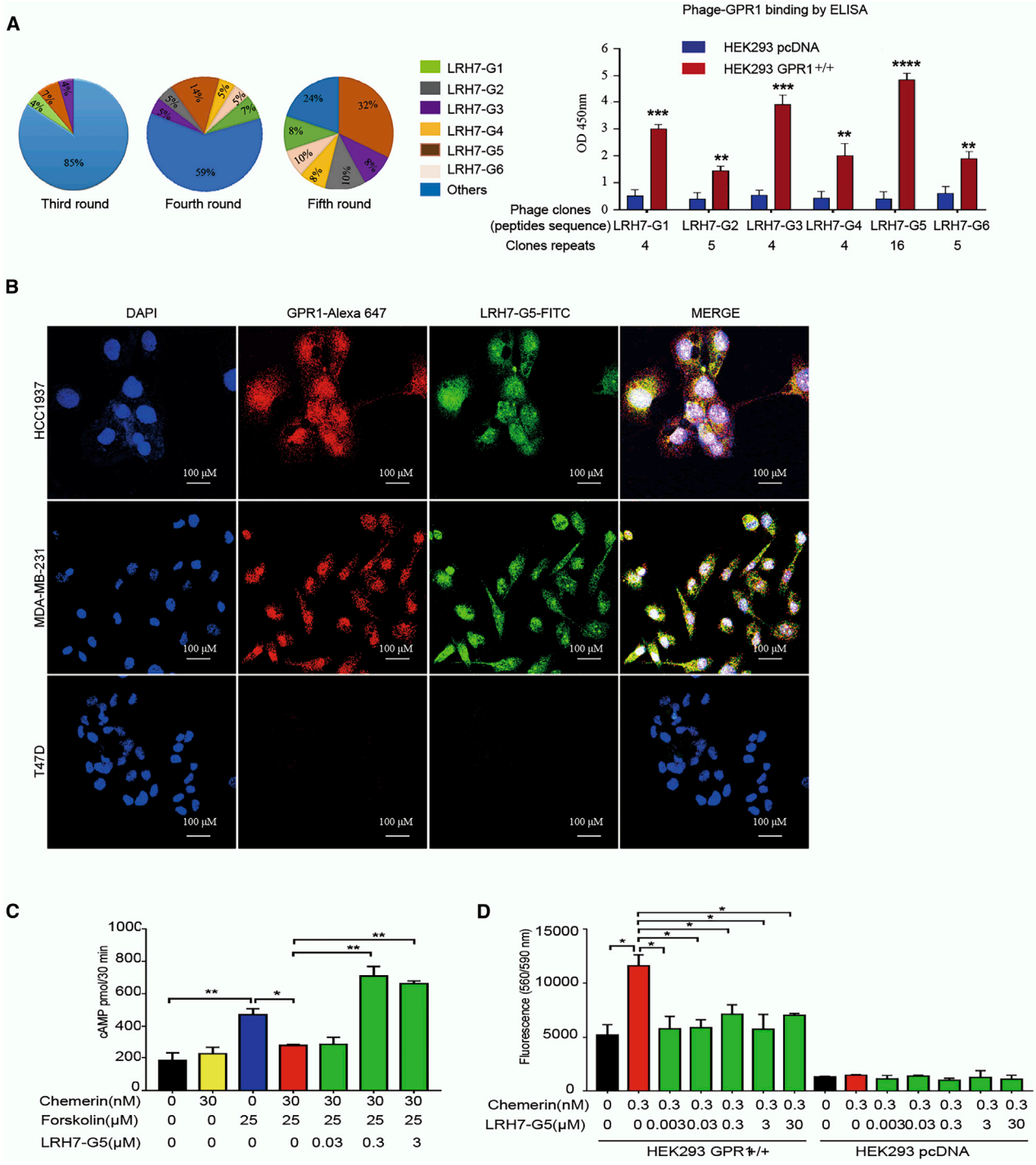

Figure 2. Identification and Characterization of GPR1-Binding Phage Peptides

(A) Peptide sequence summaries from each rounds of phage selection and the phage clones binding array to GPR1 by ELISA. **p < 0.01, ***p < 0.001, ***p < 0.0001 versus HEK293 pcDNA cells. (B) Cellular localization of peptide LRH7-G5 (1 μM) and GPR1 in breast cancer cell. (C) The stimulation of forskolin with chemerin or LRH7-G5 in cAMP production in wild HEK293 pcDNA cells. (D) The antagonist activity of LRH7-G5 for chemerin was assessed using a calcium-mobilization assay. The results are representative of three independent experiments and are expressed as the mean ± SD. *p < 0.05, **p < 0.01.

these results suggest that LRH7-G5 can specifically interact with GPR1 and inhibit chemerin/GPR1 signaling.

Binding of LRH7-G5 with GPR1 Inhibits the Growth and Induces the Death of TNBC Cells

To assess the effect of peptide LRH7-G5 on TNBC cells, we examined the proliferation curves of the MDA-MB-231, HCC1937, and T47D cell lines. As shown in Figure 3A, LRH7-G5 significantly suppressed cell growth in a dose-dependent manner in the TNBC cell lines MDA-MB-231 and HCC1937 but has little effect on T47D cell line. Comparable results were observed in the Edu staining assay (Figures S2A–S2C). This peptide-specific effect on the TNBC cell lines was validated by colony formation assays after treatment of MDA-MB-231 (Figure 3B) and HCC1937 cells with different concentrations of LRH7-G5 for 1 month (Figure S2D). Furthermore, we found that LRH7-G5 treatment arrested MDA-MB-231 cells at the G0/G1 phase boundary (Figure 3C) and induced their apoptosis (Figure 3D; Figures S3A–S3F), indicating that GPR1 signaling is required for the survival and/or proliferation of TNBC cells.

Effect of LRH7-G5 on TNBC Cell Invasion and Migration and Identification of the Involved Signaling Pathways

As shown in Figures 4A–4C, the invasion and migration of TNBC cells (MDA-MB-231 and HCC1937) were significantly suppressed by LRH7-G5 in a dose-dependent manner (Figures S4A–S4C). To investigate the mechanism underlying the selective effect of peptide LRH7-G5 on TNBC cells, we examined the relative expression levels of proteins involved in the cell cycle, apoptosis, and invasion. As shown in Figure 4D, the levels of the cell-cycle-related protein cyclin D and the apoptosis regulator proteins Stat3 and Bcl-2 were decreased, as were those of the invasion-related proteins N-cadherin, MMP-9, MMP-2, vimentin, and Snail. The effect of the peptide in relation to the PI3K/AKT pathway was also studied. LRH7-G5 significantly decreased the phosphorylation of AKT and ERK. When cocultured with the AKT phosphorylation activator SC-79 and the PI3K inhibitor wortmannin, the effect of the LRH7-G5 peptide was enhanced by the AKT agonist and weakened by the PI3K inhibitor.

LRH7-G5 Impairs the Growth of Breast Tumor Xenografts

To further investigate the effect of LRH7-G5 *in vitro*, we implanted of MDA-MB-231 and HCC1937 cells into nude mice and monitored tumor growth by bioluminescence imaging. As shown in Figures 5A–5E and Figures S5A–S5E (HCC1937), LRH7-G5 treatment substantially suppressed tumor growth and reduced the tumor burden in a dose-dependent manner. Importantly, the mean body weight did not change significantly (Figure 5F). Tumor tissue exhibited cellular necrosis (Figure 6A) and decreased cell growth, as indicated by staining of Ki-67, PCNA, and vimentin (Figure 6B), as well as an increase in cellular apoptosis, as shown by the TUNEL assay (Figure 6C). We also used the HCC1937 cell line to establish a nude mouse breast cancer model and found that LRH7-G5 treatment markedly decreased tumor volume and weight compared with those in the control group (Figures S5A–S5D) but did not affect body weight (Figure S5E).

DISCUSSION

The roles of chemerin in inflammation,[15–17] glucose homeostasis,[18–22] and carcinogenesis[23,24] have been established. Chemerin is considered an important regulator of tumor immune surveillance because it enhances immune cell recruitment to tumors and suppresses tumor progression. This process occurs mainly in chemerin-depleted tumors, such as squamous cell carcinoma of the skin, liver cancer, and melanoma, and is mediated by the receptor CMKLR1.[25,26] Previously, chemerin was reported to be highly expressed in malignant breast cancer and is considered an independent predictor of poor prognosis in breast cancer.[27] Forced overexpression of chemerin led to immune cell recruitment and suppressed breast cancer growth.[23] However, the role of GPR1 in cancer, especially breast cancer, remains unknown. Our study indicated that GPR1 expression is increased in breast cancer tissue and TNBC cell lines. Thus, by screening a phage display peptide library, we selected peptide LRH7-G5, which inhibited chemerin/GPR1 signaling, as an antagonist of GPR1. Treatment with this peptide antagonist significantly decreased TNBC cell growth, suggesting GPR1 as a therapeutic target for TNBC.

The peptide screened through the phage display peptide library is implicated as a powerful sequence-targeting anticancer tool.[28] Cancer chemotherapy based on peptides has historically attracted considerable interest due to the unique advantages of peptides, such as their low molecular weight, ability to specifically target tumor cells, and low toxicity to normal tissues.[29] Since the approval of sipuleucel-T by the US Food and Drug Administration (FDA) as the first standard peptide vaccine for prostate tumors, an increasing number of peptides have been tested in many other types of cancer, such as melanoma, glioblastoma, breast cancer, and gastric cancer.[30–32] In breast cancer, strategies for peptide chemotherapy have been proposed as vaccines to improve immune efficacy. For example, the modified peptide sequence PPV improves immune efficacy in TNBC patients by inducing an immune response.[33] Moreover, no patient experienced severe therapy-related adverse events during the course of treatment.[1] Another study on the HER-2-derived peptide P5 encapsulated in a delivery system showed produced an elevated specific cytotoxic T lymphocyte (CTL) response in mice inoculated with TUBO tumor cells.[34] A synthetic long peptide consisting of survivin-18 (SU18) and SU22 connected by a glycine linker induced interferon–γ (IFN-γ)-producing Th1 and Tc1 cells in tumor tissue,[31] and a granulocyte-macrophage colony-stimulating factor (GM-CSF)-derived peptide combined with E75 was shown to inhibit tumor recurrence.[35] Furthermore, the multipeptides derived from an ErbB-2 vaccine suppressed the growth of breast stem cells and consequently prevented tumorigenesis.[36] Similarly, GPR1, as a chemerin receptor, is highly expressed in breast cancer tissue. Our screened peptide LRH7-G5 acts as an antagonist to disrupt tumor cell growth, suggesting that it is a promising cancer therapeutic tool.

A number of chemerin-derived peptides have been investigated, such as the peptide chemerin-9 (having the 9 amino acid sequence ^{149}YFPGQYFPGQFAFS^{157}, C9), which has historically been regarded to act as an agonist of the chemerin receptor.[37] The binding affinities

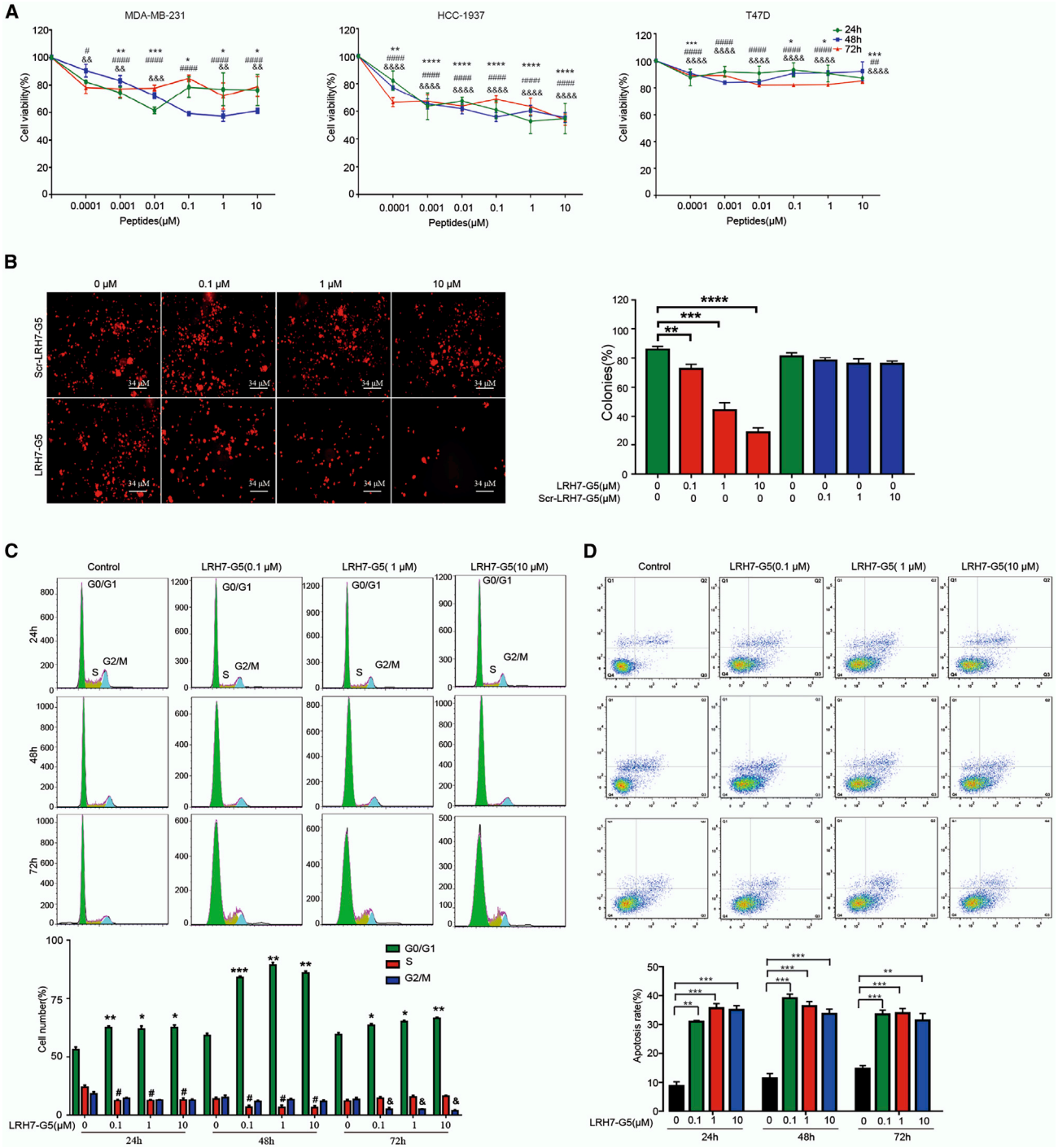

Figure 3. LRH7-G5 Combined with GPR1 Inhibits TNBC Cells' Growth and Induces Cell Deaths

(A) MDA-MB-231, HCC-1937, and T47D cells were seeded into 96-well plates and then treated with various concentrations (1 nM–100 μM) of peptides for 24, 48, or 72 h. Cell viability was determined using MTT assay. Statistical significance was calculated with one-way ANOVA, * compared with 0 μM on 24 h, # compared with 0 μM on 48 h, and compared with 0 μM on 72 h. (B) Colony formation of MDA-MB-231 after 1 month of treatment with peptides LRH7-G5 or SCRLRH7-G5 with indicated concentration. (C) MDA-MB-231 cells was treated with the indicated concentrations of LRH7-G5 at 24, 48, or 72h. Cell-cycle distribution was measured using flow cytometry. *$p < 0.05$, **$p < 0.01$, ***$p < 0.001$ was versus G0/G1 phase in control group, #$p < 0.05$ was versus S phase in control group, and &$p < 0.05$ was versus G2/M phase in control group. (D) MDA-MB-231 cells was stimulated with indicated concentrations of LRH7-G5 at 24, 48, or 72 h, and were then co-stained with PI and FITC-conjugated Annexin V. All the results are representative of three independent experiments and are expressed as the mean ± SD. *$p < 0.05$, **$p < 0.01$, ***$p < 0.001$, ****$p < 0.0001$.

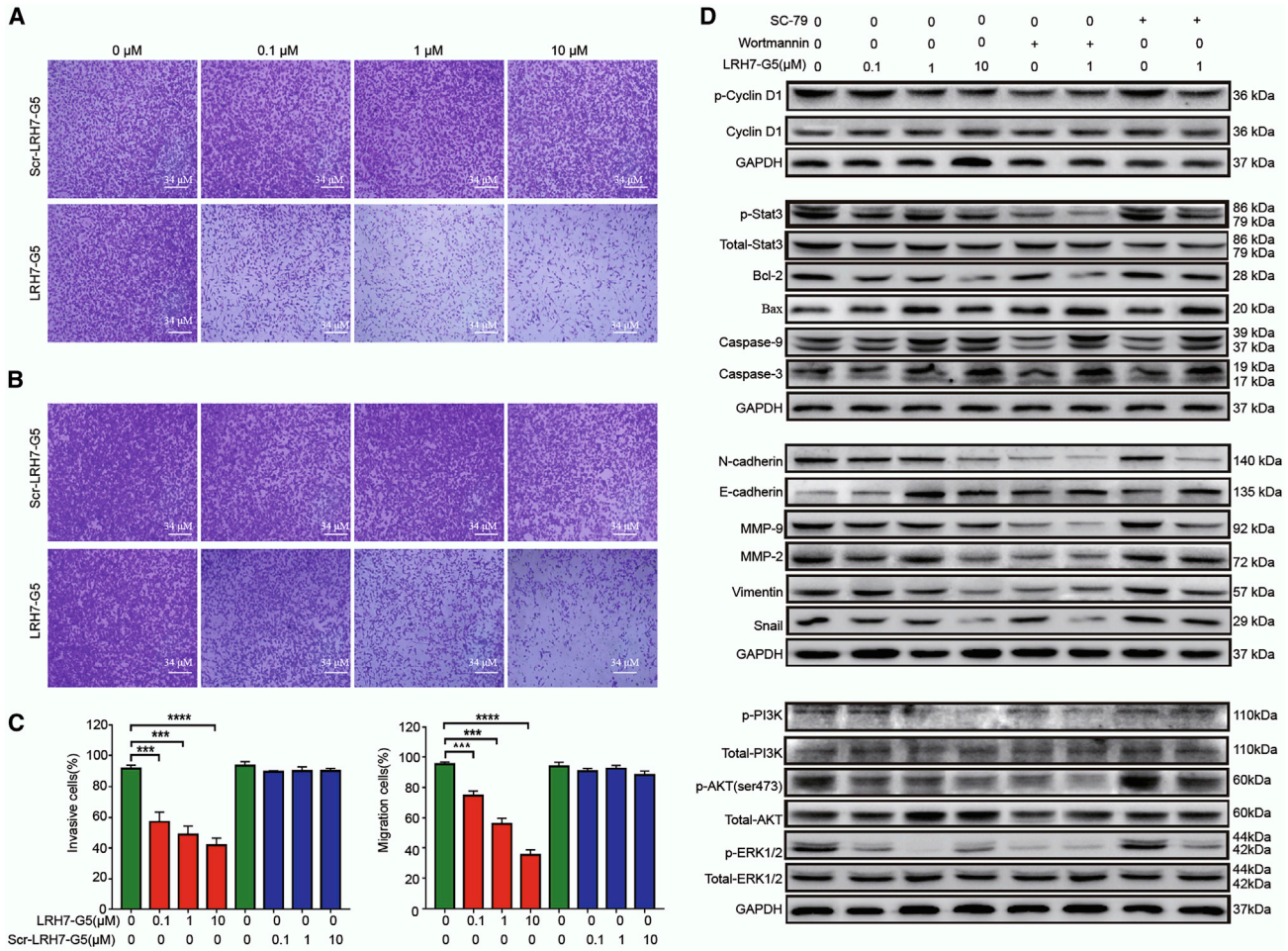

Figure 4. LRH7-G5 Decreased Invasive, Migration, and Colony Formation in TNBC Cells

(A) Boyden chamber Transwell invasion assays of MDA-MB-231 were performed in chambers pre-coated with Matrigel (×200). (B) LRH7-G5 decreased migration in MDA-MB-231 were treated with LRH7-G5 for the various concentration. (C) The cell number for invasion and migration were calculated. the results are representative of three independent experiments and are expressed as the mean ± SD.*$p < 0.05$, **$p < 0.01$, ***$p < 0.001$, ****$p < 0.0001$. (D) Immunoblots were performed on cell lysates with the indicated antibodies.

of chemerin and its derived peptides for the receptors CMKLR1 and GPR1 are similar, and this binding triggers receptor internalization, subsequent C-FOS expression, and cAMP production.[11,38] Kinetic analysis of our selected GPR1 peptide LRH7-G5 showed that this peptide had a binding affinity similar to that of the chemerin-derived peptide C20 in breast cell lines. More importantly, LRH7-G5 showed marked colocalization with GPR1 in breast cancer, attenuated chemerin-stimulated cAMP production, and calcium release, and functioned differently than the chemerin-derived peptides C9 and C20, indicating that LRH7-G5 functions as an antagonist of chemerin in chemerin/GPR1 signaling. In summary, our study provides evidence that the GPR1 antagonist peptide LRH7-G5 has an antitumor effect on TNBC and suggests that this peptide is a promising therapeutic target in basal-like TNBC cancers. Moreover, our study provides an underlying mechanism explaining how GPR1 regulates TNBC cell proliferation.

MATERIALS AND METHODS

Ethics Approval and Consent to Participate

All tumor tissues from patients were obtained from Peking University Shenzhen Hospital. The collection and use of human specimens in this study were approved by the Institutional Review Board of Shenzhen Institute of Advanced Technology, Chinese Academy of Sciences. All procedures in studies involving human participants were performed in accordance with the ethical standards of the institutional research committee and with the 1964 Declaration of Helsinki and its later amendments or comparable ethical standards.

Plasmids and Reagents

The human GPR1 (NM_001098199.1) expression vector and empty control vector (pcDNA3.0) with the G418 (geneticin) resistance gene were kind gifts from Dr. Brian Zabel and Dr. Eugene Butcher

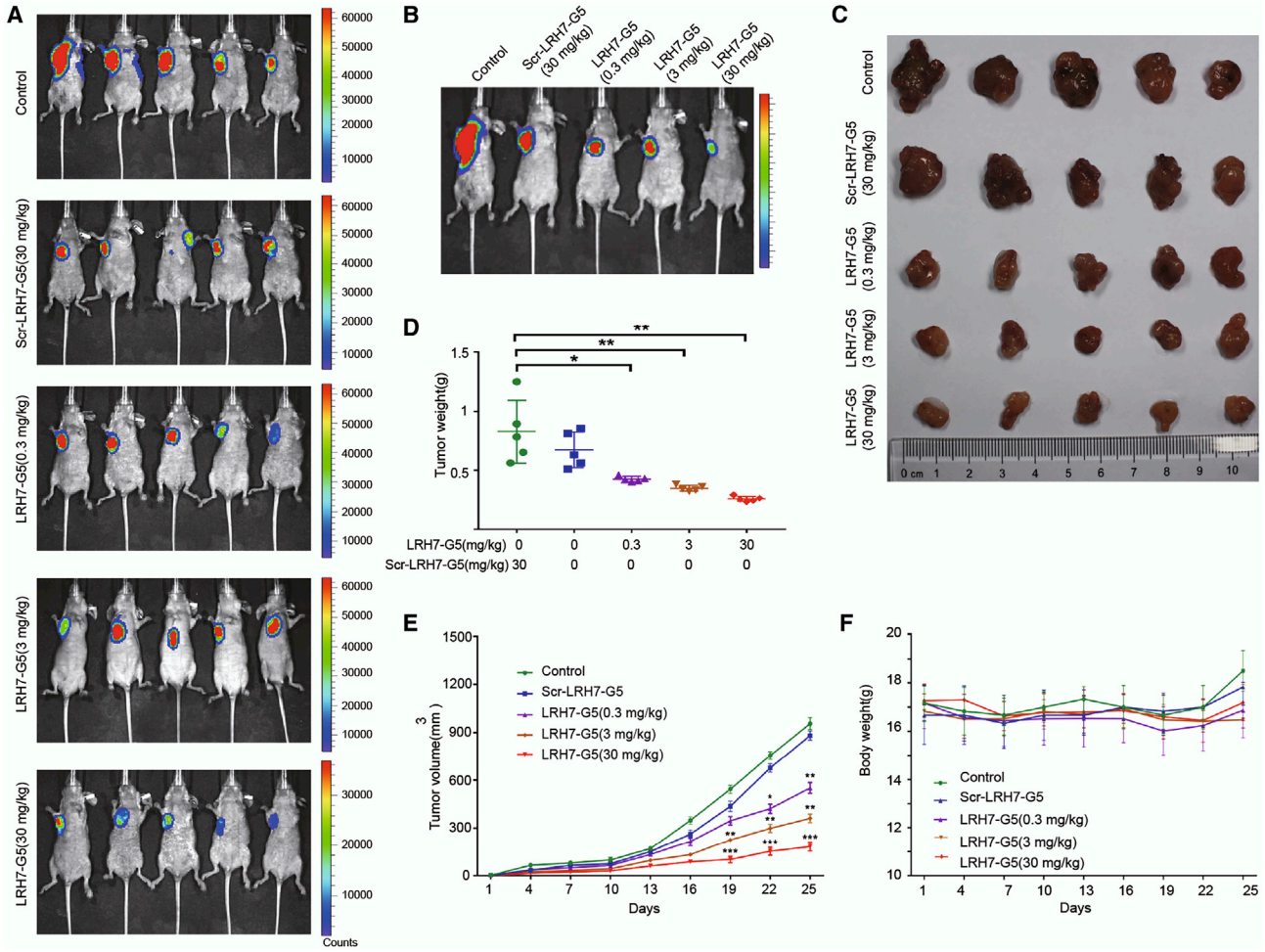

Figure 5. LRH7-G5 Suppresses Breast Cancer Tumorigenesis *In Vivo*

(A and B) Bioluminescence imaging of tumor growth. (C–E) Tumor weight and volume for LRH7-G5 or scr-LRH7-G5 treatment (n = 5–6 for each group). The tumor weight and tmor volume are expressed as the mean ± SD. P value is compared with control group, *p < 0.05, **p < 0.01, ***p < 0.001. (F) Effect of LRH7-G5 or scr-LRH7-G5 on body weight. The results are representative of three independent experiments and are expressed as the mean ± SD. *p < 0.05, **p < 0.01, ***p < 0.001.

(Stanford University, USA). Human recombinant chemerin was purchased from R&D Systems (Minneapolis, MN, USA). The LRH7-G5(MPRLPPA), human C-20 (huC-20, VQRAGEDPHSFYFPGQ FAFS), and the scramble peptide for LRH7-G5 (Scr-LRH7-G5, RLPMPAP) were synthesized by GL Biochem (Shanghai, China).

Cell Culture and Transfection

The MDA-MB-231, HCC1937, T47D, BT549, MCF-7, and HEK293 cell lines and the human mammary epithelial cell line MCF-10A were purchased from the American Type Culture Collection (ATCC). Cells were grown in DMEM (MDA-MB-231, MCF-7, HCC1937, and HEK293) or RPMI (T47D and BT549) supplemented with 10% FBS. MCF-10A cells were maintained in MEBM (Lonza) supplemented with 100 ng/mL cholera toxin (Sigma) and MEGM SingleQuot (Lonza) supplemented with GA-1000 (a gentamycin–amphotericin B mixture). All cell lines were maintained at 37°C in a humidified atmosphere of 5% CO_2 before experiments. The Lipofectamine 2000 transfection reagent (Invitrogen) was used to obtain stable GPR1-overexpressing HEK293 cells (HEK293 GPR1$^{+/+}$ cells), and the pcDNA3.0 empty vector was used as a control (HEK293 pcDNA cells).

Peptide Selection by Screening of a Phage Display Peptide Library

The Ph.D.-7 Phage Display Peptide Library with a diversity of 2.8×10^9 was used to select GPR1-binding phage clones, as previously reported.[39] In brief, HEK293 GPR1$^{+/+}$ and HEK293 pcDNA cells, which were generated via transfection of the pcDNA3.0-GPR1 and pcDNA3.0 vectors, respectively, were seeded in 6-well plates (2×10^5 cells/well) for 24 h. GPR1-binding phage clones were enriched by panning the precleared phage library over HEK293 GPR1$^{+/+}$ cells. After five rounds of elution and neutralization, the selected phage clones were serially diluted and cocultured with HEK293 GPR1$^{+/+}$ or HEK293 pcDNA

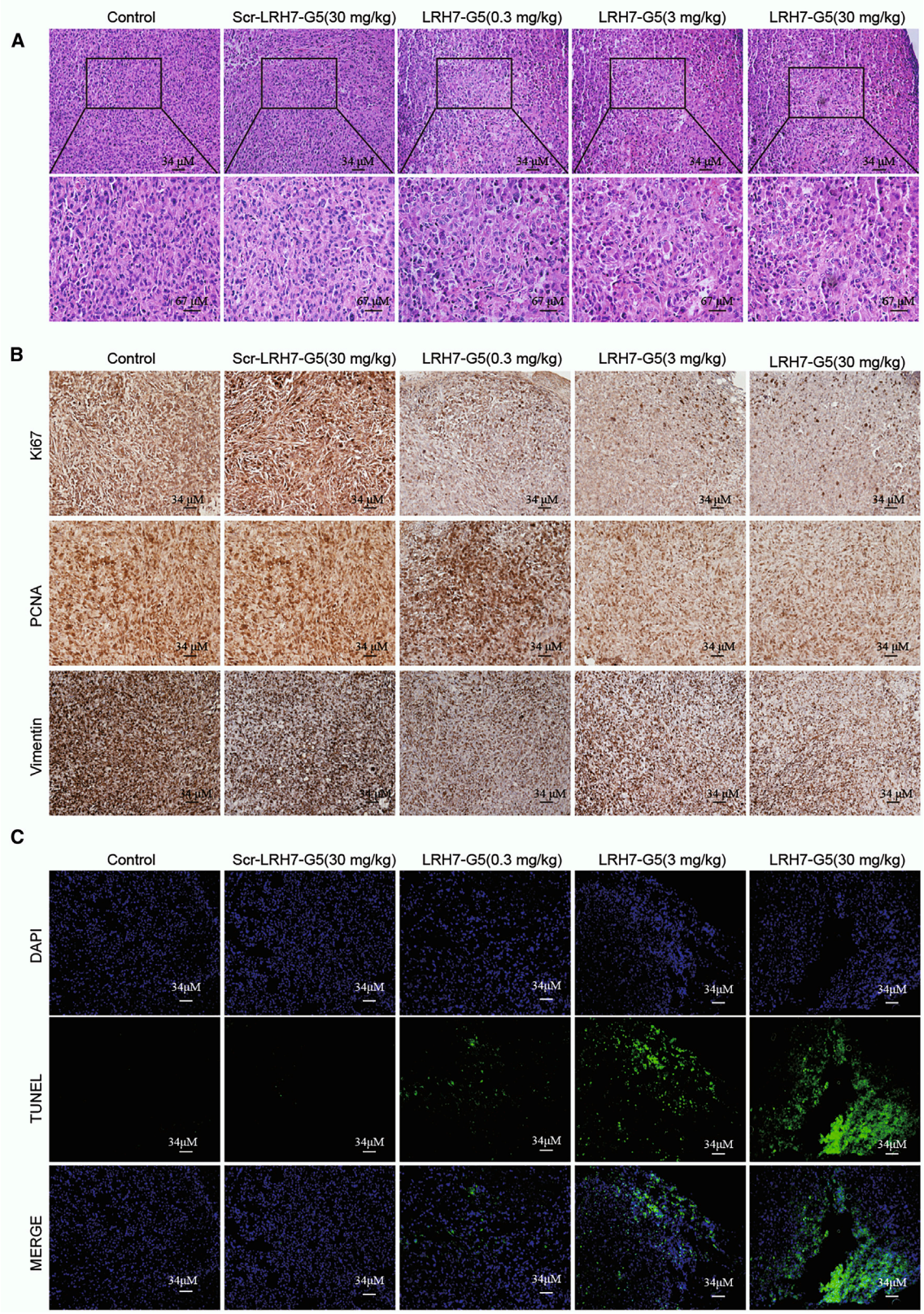

(legend on next page)

Table 1. Sequences of Primers Used in qPCR Experiments

Gene	Primers sequences
Human *β-actin*	Forward: 5′-AGCGAGCATCCCCCAAAGTT-3′
	Reverse: 5′-GGGCACGAAGGCTCATCATT-3′
Human *GPR1*	Forward: 5′-GGAGCTCAGCATTCATCACA-3′
	Reverse: 5′-GACAGGCTCTTGGTTT CAGC-3′

cells. Finally, the single-stranded DNAs (ssDNAs) from phage clones were extracted and sequenced by Invitrogen Biotechnology Company (Shanghai, China). The six candidate peptides (LRH7-G1-6, translated from the positive phage clone's DNA sequence) and the scrambled control Scr-LRH7-G5 peptide were synthesized and labeled with fluorescein isothiocyanate (FITC) or biotinylated by China Peptides (Shanghai, China). High-performance liquid chromatography (HPLC) and mass spectrometry (MS) were used to confirm 98% purity of the LRH7-G5 peptide, which is approved and protected by a Chinese patent (no. 201711376678).

Peptide: GPR1 Binding Assays

First, the purified LRH7-G5 and Scr-LRH7-G5 peptides were biotinylated. The HEK293 GPR1$^{+/+}$ or HEK293 pcDNA cells were seeded in 96-well plates (5×10^3 cells/well) for 24 h. After washing three times with PBS, the plates were fixed with 4% paraformaldehyde at RT for 15 min, blocked with 5% BSA in PBS, and then treated with varying concentrations of biotinylated- LRH7-G5 or biotinylated-Scr-LRH7-G5 for 2 h at room temperature (RT). To remove the unbound peptide, we washed the plates with three times with PBS and then added the HRP-streptavidin and incubated for 1 h at RT. The substrate (50 μL/well of 3, 30, 5, 50-tetramethyl-benzidine; TMB) was added and incubated at RT for 30 min in the dark, 2 M H_2SO_4 was used to terminate the reaction, and the absorbance was measured at 450 nm. The saturation curves and scatchard plots were generated and half-saturation points (dissociation constant; Kd) were calculated by Prism software (GraphPad, La Jolla, CA).

Immunofluorescence Staining for Peptides

MDA-MB-231, HCC1937, and T47D cells were incubated with 1 μM FITC-labeled LRH7-G5 peptide for 2 h at RT, and Scr-LRH7-G5 was used as a control. After staining with 4′,6-diamidino-2-phenylindole (DAPI) for 5 min, images were acquired by confocal microscopy (LSM 700, Carl Zeiss, Germany) using a 60× oil objective lens. Colocalization of LRH7-G5 peptides and GPR1 in cells was also assessed as described.[40]

cAMP Assay and Calcium Mobilization Assay

HEK293 GPR1$^{+/+}$ and HEK293 pcDNA cells were seeded in 6-well plates (5×10^3 cells/well) for 24 h and were then incubated for 30 min at 37°C with 10 nM huChemerin, 10 μM forskolin (Sigma, St. Louis, MO, USA), serial dilutions of LRH7-G5, a combination of forskolin and huChemerin, or a combination of forskolin, huChemerin, and peptides. Then, the cells were subjected to a cAMP assay with a kit obtained from R&D System. The calcium mobilization assay was performed using Fluo-4 NW Calcium Assay Kits (Thermo Fisher Scientific, Rockford, IL, USA), and the protocol was performed following the manufacturer's instructions.

Quantitative Real-Time PCR Assays

RNA was isolated from breast cancer tissue and cell lines by using TRIzol Reagent (Invitrogen) according to the manufacturer's protocol, as previously described.[41] RNA samples were reverse transcribed to cDNA, and the relative transcript abundances were then estimated by quantitative real-time PCR using a SYBR RT-PCR kit (Takara, Shiga, Japan) according to the manufacturer's instructions. The $2^{-\Delta\Delta Ct}$ method was used to calculate the relative gene expression levels, which were normalized to those of beta-actin. The primer sequences are listed in Table 1.

Western Blot Analysis

Total protein was harvested from cells and breast cancer tissues. The following primary antibodies were used: phospho-PI3K (CST, #4228), PI3K (CST, #4292), phospho-AKT (Ser473; Abcam, ab66138), AKT (CST, #4691), phospho-ERK1/2 (CST, #4370), ERK1/2 (CST, #4695), phospho-Cyclin D1 (CST, #3300), Cyclin D1 (CST, #2978), phospho-Stat3 (CST, #9145), Stat3 (CST, #12640), Snail (CST, #3879), Bax (Abcam, ab53154), Bcl-2 (CST, #4223), E-cadherin (CST, #3195), N-cadherin (CST, #14215), MMP-2 (CST, #87809), MMP-9 (CST, #13667), Vimentin (Abcam, ab92547), Caspase-3 (Abcam, ab4051), and Caspase-9 (Abcam, ab2014).

Colorimetric MTT Assay

Cells in the logarithmic growth phase were seeded in 96-well plates (5×10^3 cells/well) for 24 h, starved with 0.04% FBS medium for another 12 h, and then treated with serially diluted LRH7-G5 or Scr-LRH7-G5 peptides (0.04% FBS medium) for 24, 48, and 72 h. Cell viability was determined using the methylthiazole tetrazolium (MTT) method.

Flow Cytometry and Plate Colony Formation Assay

After treatment with serially diluted LRH7-G5 or Scr-LRH7-G5 peptides for 24, 48, and 72 h, cells were subsequently stained with propidium iodide (PI) in the dark for 30 min at RT, and the percentages of cells in the G0/G1, S, and G2/M phases were then determined (BD Biosciences, Franklin Lakes, NJ) according to the manufacturer's protocol. Annexin V^+/PI^- (early apoptotic) and Annexin V^+/PI^+ (late apoptotic) cells were considered the apoptotic portion.

MDA-MB-231-tomato and HCC1937-tomato cells were seeded in a 6-well plate (1×10^3 cells/well) and stimulated as indicated. After

Figure 6. LRH7-G5 Promoted Cancer Cells Apoptosis *In Vivo*

(A) H&E staining for LRH7-G5 or scr-LRH7-G5 treatment. Upper (×200) and down (×400). (B) Immunohistochemistry (IHC) staining for Ki-67, PCNA, and vimentin (×200). (C) LRH7-G5 induces apoptosis in tumors, as determined by TUNEL assay (×200).

incubation for 3 weeks, the colonies in the plates were large enough to be visualized. Images of each well were acquired and used to quantitate growth by counting colonies under a fluorescence microscope (Olympus fluorescence microscope, Japan).

Cell Migration and Invasion Assay

The migration assay was performed with Transwell chambers without Matrigel (Corning Costar) according to the manufacturer's protocol. MDA-MB-231 cells were seeded into the upper chamber with FBS-free medium or serially diluted LRH7-G5 or Scr-LRH7-G5 peptide (0.1 μM to 10 μM), 10% FBS medium was added to the lower chamber as chemoattractant. The plates containing chambers were incubated at 37°C in 5% CO_2 for 12 h. Non-migration cells on the surface of the upper chambers were then gently removed. The migrating cells on the surface of the lower chambers were fixed in methanol for 10 min, stained with hematoxylin for 30 min at RT. Cell numbers were quantified and the images were captured under inverted microscope (Olympas, Center Valley, PA).

Cell invasion was also studied with Transwell chambers containing Matrigel (Matrigel, BD Biosciences). MDA-MB-231 and HCC1937 cells (2×10^4 cell) were seeded into the upper chamber with matrigel in FBS-free medium and serum-free medium with serially diluted LRH7-G5 or Scr-LRH7-G5 peptides, 10% FBS medium was added to the lower chamber as chemoattractant. The plates containing chambers were incubated at 37°C in 5% CO_2 for 48 h (Olympas, Center Valley, PA). The images were taken and evaluated as migration method described here.

Animal Study

25 female, nude BALB/c mice (4–6 weeks of age) were obtained from Beijing Vital River Laboratory Animal Technology (Beijing, China), randomly divided into five groups, and subcutaneously injected with MDA-MB-231-tomato or HCC1937-tomato cells (7×10^6 cells in 100 μL PBS/mouse) into the left axilla. The mice were then intraperitoneally injected with serially diluted LRH7-G5 or Scr-LRH7-G5 peptides daily. The body weight and tumor sizes were recorded every 3 days. Primary tumor volume was calculated with the formula: (length) × $(\text{width})^2 \times 0.5$. After 25 days treatment, the mice were sacrificed, and the tumor tissues were collected for further experiments. The IVIS imaging was used to monitor tumor development twice a week with IVIS spectrum instrument (Perkin Elmer). Animal welfare and experimental procedures were approved by the Committee on the Use of Live Animals for Teaching and Research, Shenzhen Institutes of Advanced Technology, Chinese Academy of Sciences, and were carried out in strict accordance with the related regulations. All applicable institutional guidelines for the care and use of animals were followed.

Staining and TUNEL Assay

The tissue samples were fixed in 4% PFA overnight and embedded in paraffin. After sectioning, staining against Ki67 (Abcam, ab15580), PCNA (Abcam, ab29), Vimentin (Abcam, ab92547), and MMP-9(CST, #13667) were performed using immunohistochemistry kit (Key-GEN, Nanjing, China). The FragEL DNA Fragmentation Detection Kit (Calbiochem, Germany) was used to detect the apoptosis cells in tumor tissue.

Statistics

All the results are presented as the mean ± SD with at least three independent experiments. Statistical analyses were performed with one-way ANOVA (GraphPad Prism 6.0) for multiple groups. The threshold of $p < 0.05$ was defined as statistically significant.

SUPPLEMENTAL INFORMATION

Supplemental Information can be found online at https://doi.org/10.1016/j.omto.2020.08.013.

AUTHOR CONTRIBUTIONS

C.H. and X.Y.D. conducted literature search, figure and study design, data collection, and analysis and article writing and contributed equally to the research. J.X.C. and B.B.W. cultured the cells and worked on the *in vitro* experiments. J.C. and W.Z. were involved in animal work, mouse model use, and mice data collection. E.W. contributed to draft revision and polishing. W.W. and J.V.Z. were corresponding authors; both conceived and designed the experiments, interpreted data, and revised the draft, contributing to the article equally. Otherwise, it is gratful for Z.L.X (not listed as author)' contribution to Graphic abstract design and polish.

CONFLICTS OF INTEREST

The authors declare no competing interests.

ACKNOWLEDGMENTS

This work was supported by National Key Research and Development Program of China (2018YFC1003703), National Nature Science Foundation of China (NSFC; 81901509, 31671562 ,81830041), China Postdoctoral Science Foundation Funded Project (2018M640843), Shenzhen grant (JCYJ20170815090309586, JCYJ20170817143406822, and JCYJ20190812165809537), and Shenzhen Key Medical Discipline Construction Fund (number SZXK017). The corresponding author W.W. and J.V.Z. had the full access to all the data in the study and had final responsibility for the decision to submit for publication.

REFERENCES

1. Albrethsen, J., Møller, C.H., Olsen, J., Raskov, H., and Gammeltoft, S. (2006). Human neutrophil peptides 1, 2 and 3 are biochemical markers for metastatic colorectal cancer. Eur. J. Cancer *42*, 3057–3064.
2. Ginsburg, O., Bray, F., Coleman, M.P., Vanderpuye, V., Eniu, A., Kotha, S.R., Sarker, M., Huong, T.T., Allemani, C., Dvaladze, A., et al. (2017). The global burden of women's cancers: a grand challenge in global health. Lancet *389*, 847–860.
3. Sari, E., and Yalcin, S. (2016). Clinical Aspects of Estrogen and Progesterone Receptors and ERBB2 Testing. In Breast Disease, A. Aydiner, A. Igci, and A. Soran, eds., pp. 143–161, Springer.
4. Bauer, K.R., Brown, M., Cress, R.D., Parise, C.A., and Caggiano, V. (2007). Descriptive analysis of estrogen receptor (ER)-negative, progesterone receptor (PR)-negative, and HER2-negative invasive breast cancer, the so-called triple-negative phenotype: a population-based study from the California cancer Registry. Cancer *109*, 1721–1728.
5. Brewster, A.M., Chavez-MacGregor, M., and Brown, P. (2014). Epidemiology, biology, and treatment of triple-negative breast cancer in women of African ancestry. Lancet Oncol. *15*, e625–e634.

6. Bianchini, G., Balko, J.M., Mayer, I.A., Sanders, M.E., and Gianni, L. (2016). Triple-negative breast cancer: challenges and opportunities of a heterogeneous disease. Nat. Rev. Clin. Oncol. *13*, 674–690.

7. Garrido-Castro, A.C., Lin, N.U., and Polyak, K. (2019). Insights into Molecular Classifications of Triple-Negative Breast Cancer: Improving Patient Selection for Treatment. Cancer Discov. *9*, 176–198.

8. Yang, Y.L., Ren, L.R., Sun, L.F., Huang, C., Xiao, T.X., Wang, B.B., Chen, J., Zabel, B.A., Ren, P., and Zhang, J.V. (2016). The role of GPR1 signaling in mice corpus luteum. J. Endocrinol. *230*, 55–65.

9. Rourke, J.L., Muruganandan, S., Dranse, H.J., McMullen, N.M., and Sinal, C.J. (2014). Gpr1 is an active chemerin receptor influencing glucose homeostasis in obese mice. J. Endocrinol. *222*, 201–215.

10. Wittamer, V., Franssen, J.D., Vulcano, M., Mirjolet, J.F., Le Poul, E., Migeotte, I., Brézillon, S., Tyldesley, R., Blanpain, C., Detheux, M., et al. (2003). Specific recruitment of antigen-presenting cells by chemerin, a novel processed ligand from human inflammatory fluids. J. Exp. Med. *198*, 977–985.

11. Li, L., Huang, C., Zhang, X., Wang, J., Ma, P., Liu, Y., Xiao, T., Zabel, B.A., and Zhang, J.V. (2014). Chemerin-derived peptide C-20 suppressed gonadal steroidogenesis. Am. J. Reprod. Immunol. *71*, 265–277.

12. Jinno-Oue, A., Shimizu, N., Soda, Y., Tanaka, A., Ohtsuki, T., Kurosaki, D., Suzuki, Y., and Hoshino, H. (2005). The synthetic peptide derived from the NH2-terminal extracellular region of an orphan G protein-coupled receptor, GPR1, preferentially inhibits infection of X4 HIV-1. J. Biol. Chem. *280*, 30924–30934.

13. Kumar, J.D., Aolymat, I., Tiszlavicz, L., Reisz, Z., Garalla, H.M., Beynon, R., Simpson, D., Dockray, G.J., and Varro, A. (2019). Chemerin acts via CMKLR1 and GPR1 to stimulate migration and invasion of gastric cancer cells: putative role of decreased TIMP-1 and TIMP-2. Oncotarget *10*, 98–112.

14. Lee, J.H., Jung, S.M., Yang, K.M., Bae, E., Ahn, S.G., Park, J.S., Seo, D., Kim, M., Ha, J., Lee, J., et al. (2017). A20 promotes metastasis of aggressive basal-like breast cancers through multi-monoubiquitylation of Snail1. Nat. Cell Biol. *19*, 1260–1273.

15. Parlee, S.D., Ernst, M.C., Muruganandan, S., Sinal, C.J., and Goralski, K.B. (2010). Serum chemerin levels vary with time of day and are modified by obesity and tumor necrosis factor-alpha. Endocrinology *151*, 2590–2602.

16. Bondue, B., Wittamer, V., and Parmentier, M. (2011). Chemerin and its receptors in leukocyte trafficking, inflammation and metabolism. Cytokine Growth Factor Rev. *22*, 331–338.

17. Fülöp, P., Seres, I., Lőrincz, H., Harangi, M., Somodi, S., and Paragh, G. (2014). Association of chemerin with oxidative stress, inflammation and classical adipokines in non-diabetic obese patients. J. Cell. Mol. Med. *18*, 1313–1320.

18. Aursulesei, V., Anisie, E., Alecsa, A.M., Constantin, M.M.L., and Al Namat, R. (2017). Circulating Chemerin is Associated with Subclinical Atherosclerosis in Obesity. Rev Chim-Bucharest *68*, 541–544.

19. Niklowitz, P., Rothermel, J., Lass, N., Barth, A., and Reinehr, T. (2018). Link between chemerin, central obesity, and parameters of the Metabolic Syndrome: findings from a longitudinal study in obese children participating in a lifestyle intervention. Int. J. Obes. *42*, 1743–1752.

20. Buechler, C., Feder, S., Haberl, E.M., and Aslanidis, C. (2019). Chemerin Isoforms and Activity in Obesity. Int. J. Mol. Sci. *20*, 1128.

21. Ernst, M.C., Issa, M., Goralski, K.B., and Sinal, C.J. (2010). Chemerin exacerbates glucose intolerance in mouse models of obesity and diabetes. Endocrinology *151*, 1998–2007.

22. Horn, P., Metzing, U.B., Steidl, R., Romeike, B., Rauchfuß, F., Sponholz, C., Thomas-Rüddel, D., Ludewig, K., Birkenfeld, A.L., Settmacher, U., et al. (2016). Chemerin in peritoneal sepsis and its associations with glucose metabolism and prognosis: a translational cross-sectional study. Crit. Care *20*, 39.

23. Pachynski, R.K., Wang, P., Salazar, N., Zheng, Y., Nease, L., Rosalez, J., Leong, W.I., Virdi, G., Rennier, K., Shin, W.J., et al. (2019). Chemerin Suppresses Breast Cancer Growth by Recruiting Immune Effector Cells Into the Tumor Microenvironment. Front. Immunol. *10*, 983.

24. Lin, W., Chen, Y.L., Jiang, L., and Chen, J.K. (2011). Reduced expression of chemerin is associated with a poor prognosis and a lowed infiltration of both dendritic cells and natural killer cells in human hepatocellular carcinoma. Clin. Lab. *57*, 879–885.

25. Kumar, J.D., Kandola, S., Tiszlavicz, L., Reisz, Z., Dockray, G.J., and Varro, A. (2016). The role of chemerin and ChemR23 in stimulating the invasion of squamous oesophageal cancer cells. Br. J. Cancer *114*, 1152–1159.

26. Pachynski, R., Zabel, B., Kohrt, H., Tejeda, N.M., Monnier, J., Swanson, C., Holzer, A.K., Gentles, A., Sperinde, G.V., Edalati, A., et al. (2013). The chemoattractant chemerin suppresses melanoma by recruiting natural killer cell antitumor defenses. Cancer Res. *209*, 73.

27. El-Sagheer, G., Gayyed, M., Ahmad, A., Abd El-Fattah, A., and Mohamed, M. (2018). Expression of chemerin correlates with a poor prognosis in female breast cancer patients. Breast Cancer (Dove Med. Press) *10*, 169–176.

28. Boohaker, R.J., Lee, M.W., Vishnubhotla, P., Perez, J.M., and Khaled, A.R. (2012). The use of therapeutic peptides to target and to kill cancer cells. Curr. Med. Chem. *19*, 3794–3804.

29. Liu, X., Peng, J., He, J., Li, Q., Zhou, J., Liang, X., and Tang, S. (2018). Selection and identification of novel peptides specifically targeting human cervical cancer. Amino Acids *50*, 577–592.

30. Zanetti, J.S., Soave, D.F., Oliveira-Costa, J.P., da Silveira, G.G., Ramalho, L.N., Garcia, S.B., Zucoloto, S., and Ribeiro-Silva, A. (2011). The role of tumor hypoxia in MUC1-positive breast carcinomas. Virchows Arch. *459*, 367–375.

31. Ohtake, J., Ohkuri, T., Togashi, Y., Kitamura, H., Okuno, K., and Nishimura, T. (2014). Identification of novel helper epitope peptides of Survivin cancer-associated antigen applicable to developing helper/killer-hybrid epitope long peptide cancer vaccine. Immunol. Lett. *161*, 20–30.

32. Margus, H., Padari, K., and Pooga, M. (2012). Cell-penetrating peptides as versatile vehicles for oligonucleotide delivery. Mol. Ther. *20*, 525–533.

33. Takahashi, R., Toh, U., Iwakuma, N., Takenaka, M., Otsuka, H., Furukawa, M., Fujii, T., Seki, N., Kawahara, A., Kage, M., et al. (2014). Feasibility study of personalized peptide vaccination for metastatic recurrent triple-negative breast cancer patients. Breast Cancer Res. *16*, R70.

34. Mansourian, M., Badiee, A., Jalali, S.A., Shariat, S., Yazdani, M., Amin, M., and Jaafari, M.R. (2014). Effective induction of anti-tumor immunity using p5 HER-2/neu derived peptide encapsulated in fusogenic DOTAP cationic liposomes co-administrated with CpG-ODN. Immunol. Lett. *162* (1 Pt A), 87–93.

35. Mittendorf, E.A., Clifton, G.T., Holmes, J.P., Schneble, E., van Echo, D., Ponniah, S., and Peoples, G.E. (2014). Final report of the phase I/II clinical trial of the E75 (nelipepimut-S) vaccine with booster inoculations to prevent disease recurrence in high-risk breast cancer patients. Ann. Oncol. *25*, 1735–1742.

36. Gil, E.Y., Jo, U.H., Lee, H.J., Kang, J., Seo, J.H., Lee, E.S., Kim, Y.H., Kim, I., Phan-Lai, V., Disis, M.L., and Park, K.H. (2014). Vaccination with ErbB-2 peptides prevents cancer stem cell expansion and suppresses the development of spontaneous tumors in MMTV-PyMT transgenic mice. Breast Cancer Res. Treat. *147*, 69–80.

37. Wittamer, V., Grégoire, F., Robberecht, P., Vassart, G., Communi, D., and Parmentier, M. (2004). The C-terminal nonapeptide of mature chemerin activates the chemerin receptor with low nanomolar potency. J. Biol. Chem. *279*, 9956–9962.

38. De Henau, O., Degroot, G.N., Imbault, V., Robert, V., De Poorter, C., Mcheik, S., Galés, C., Parmentier, M., and Springael, J.Y. (2016). Signaling Properties of Chemerin Receptors CMKLR1, GPR1 and CCRL2. PLoS ONE *11*, e0164179.

39. Dai, X., Cai, C., Xiao, F., Xiong, Y., Huang, Y., Zhang, Q., Xiang, Q., Lou, G., Lian, M., Su, Z., and Zheng, Q. (2014). Identification of a novel aFGF-binding peptide with anti-tumor effect on breast cancer from phage display library. Biochem. Biophys. Res. Commun. *445*, 795–801.

40. Sun, Z., Dai, X., Li, Y., Jiang, S., Lou, G., Cao, Q., Hu, R., Huang, Y., Su, Z., Chen, M., et al. (2016). A novel Nogo-66 receptor antagonist peptide promotes neurite regeneration in vitro. Mol. Cell. Neurosci. *71*, 80–91.

41. Huang, B.B., Liu, X.C., Qin, X.Y., Chen, J., Ren, P.G., Deng, W.F., et al. (2018). Effect of High-Fat Diet on Immature Female Mice and Messenger and Noncoding RNA Expression Profiling in Ovary and White Adipose Tissue. Reprod. Sci. *26*, 1360–1372.